

Isostructural transition coupled with spin ordering in CsCuCl₃: A spatially frustrated spiral crystal lattice

V. P. Plakhty,^{1,*} J. Wosnitzer,² N. Martin,³ Ya. Marchi,³ O. P. Smirnov,¹ B. Grenier,⁴ and S. V. Gavrilov¹

¹Petersburg Nuclear Physics Institute, RAS, Gatchina, 188300 St. Petersburg, Russia

²Hochfeld-Magnetlabor Dresden (HLD), Forschungszentrum Dresden-Rossendorf, D-01314 Dresden, Germany

³Universite Joseph Fourier, Grenoble-1, 38400 Saint Martin d'Herès, France

⁴CEA-Grenoble, DRFMC/SPSMS/MDN, 38042 Grenoble Cedex 9, France

(Received 29 August 2008; revised manuscript received 4 December 2008; published 30 January 2009)

By means of single-crystal neutron diffraction, an isostructural transition is observed at the Néel temperature of CsCuCl₃, a quasi-one-dimensional antiferromagnet with a helically modulated crystal structure that is built out of six Cu²⁺ layers. Abrupt atomic displacements of about 0.01 Å minimize the ferromagnetic interlayer superexchange interaction via the path Cu-C11-Cu that enters also the antiferromagnetic path Cu-C11-C12-Cu. The latter couples only one pair of Cu²⁺ ions in each chlorine layer since all the other intralayer bonds either have much longer interatomic distances or include more than two intermediate Cl ions and, therefore, can be neglected. Thus, a spatial geometric frustration in this helically modulated stacked triangular lattice is provided by three Cu layers. Influences of the atomic displacements on the exchange energy, as well as the critical behavior of this spatially frustrated material, are discussed.

DOI: 10.1103/PhysRevB.79.012410

PACS number(s): 75.25.+z, 75.50.-y, 61.66.Fn, 61.05.fm

Highly frustrated magnetic materials with strongly competing or even completely cancelled exchange interactions attract continuous attention. One of the reasons is that in a small or zero exchange field even very weak perturbations can play a crucial role in magnetic ordering and vice versa. A strongly frustrated system, such as the classical Heisenberg antiferromagnet on a pyrochlore lattice with spins at tetrahedral vertices, does not order at any finite temperature. A tetragonal distortion of the pyrochlore tetrahedral unit has been shown to lift the degeneracy and to stabilize the collinear spin orientation.^{1,2} Recently, a family of quasi-two-dimensional (2D) materials, RMnO₃ (*R* is a rare-earth metal), with antiferromagnetically interacting Mn³⁺ ions (*S*=2) in the corners of triangles, have been extensively studied (see Ref. 3 and references therein). The ground-state configuration is attained when the nearest-neighbor (NN) spins are inclined by $\pm 2\pi/3$ to one another.

Another very well-known class of highly frustrated systems is represented by stacked triangular lattices (STLs) reviewed by Collins and Petrenko.⁴ Investigations of such spin systems have been mainly performed on hexagonal perovskites with the general formula ABX₃, where *A* is an alkali metal and *B* is a transition metal octahedrally coordinated by halogen atoms, *X*. The neighboring layers are stacked together via the octahedral faces. The superexchange interaction *J*, mostly antiferromagnetic, between the magnetic ions in the neighboring layers involves one intermediate ligand (*B-X-B*), while inside the layer, two successive ligands (*B-X-X-B*) are involved in the antiferromagnetic interaction *J'* of the NN magnetic ions in the triangular lattice, providing a geometrical frustration, such as in RMnO₃. As found experimentally,⁴ the absolute value *J'* in the hexagonal perovskites is about 2 orders of magnitude smaller than *J*, which is the main difference to RMnO₃, where *J' ≫ J*. Among the hexagonal perovskites, the quantum antiferromagnet CsCuCl₃ with Cu²⁺ spin *S*=1/2 has a helically modulated crystal structure in the temperature range of magnetic

ordering.⁵ Its unique topology is completely different from the STL family, and it is worthwhile to reconsider important structural features, mentioned in the literature⁵ and which have not been taken into account in spin-ordering studies.⁶

At high temperature, $T > T_c = 423$ K, the hexagonal unit cell of CsCuCl₃ is described by the polar space group *P6₃mc* (*Z*=2) (Ref. 7) although polarization measurements have given no conclusive evidence on the spontaneous polarization calculated from the atomic positions assuming a point-charge model.⁷ The CuCl₆ octahedra form infinite chains along the *c* axis sharing the faces as shown in Fig. 1. Since the angle of the bond Cu-Cl-Cu in a chain is close to 90° the superexchange should be ferromagnetic.⁸ These chains form a triangular lattice in the basal plane, with Cu²⁺ ions in each copper layer being coupled by antiferromagnetic exchange paths with two parallel intermediate anion-anion overlaps, Cu-C11-C12-Cu (marked by black lines in Fig. 1), which provides a geometrical frustration.

Due to the cooperative Jahn-Teller effect, a first-order phase transition occurs at *T_c*, with the new *c* axis being tripled and with each of the three local axes, ξ , η , and ζ , of an octahedron being elongated one after the other in different copper layers when propagating along the [001] direction.⁵ This leads to a small helical displacement of $u = 0.0616(3)5$ of the Cu²⁺ ions in the 6(*a*) sites of the enantiomorphic groups *P6₁22* or *P6₅22*,⁹ with the helix wave vector being $\mathbf{k} = (0, 0, 2\pi/3)$. The helical crystal structure for the *P6₁22* enantiomer is described in Fig. 2. Again the Cu²⁺ ions in the chain interact ferromagnetically via one intermediate ligand C11. However, up to now no attention has been paid to the fact that, unlike all other hexagonal perovskites, only two out of three nearest Cu²⁺ ions in each copper layer are coupled antiferromagnetically by two parallel Cu-C11-C12-Cu bonds. Additional in-plane linkage can be provided either by some other two-anion bonds with much longer interatomic distances⁵ or by bonds with an additional intermediate anion. According to the experimental data⁵ and the theoretical estimates,¹⁰ both can be neglected.

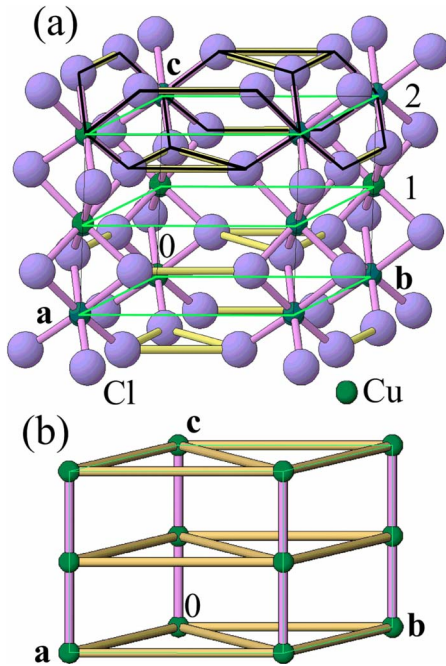


FIG. 1. (Color online) (a) Hexagonal unit cell of CsCuCl_3 in the high-temperature phase ($T > 423$ K), with the Cs^{1+} ions being omitted. The exchange paths from one Cu over two Cl ions to the neighboring Cu are marked by the black lines in one of the copper layers. (b) Each copper layer is built out of triangles with equal antiferromagnetic bonds, schematically described by the horizontal (in-plane) rods. The ferromagnetic Cu-Cl-Cu bonds between the layers are described by the vertical (inter-plane) rods.

The magnetic structure of CsCuCl_3 below the Néel temperature, $T_N = 11.7$ K, was determined by Adachi *et al.*⁶ to be a triangular spin arrangement in the basal (0,0,1) plane, with all spins being rotated by $5.1(1)^\circ$ between the nearest planes. In other words, every spin belongs to a spiral along the

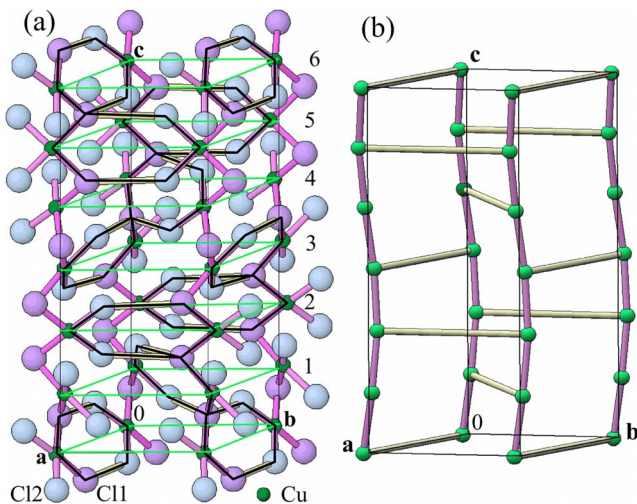


FIG. 2. (Color online) Hexagonal unit cell of CsCuCl_3 in the $P6_122$ phase below T_C . (a) All atoms, except Cs^{1+} , are shown, with the in-plane exchange bonds, Cu-Cl1-Cl2-Cu, being indicated by the black lines. (b) Schematic representation of the in-plane exchange bonds with two pairs of anion-anion overlaps.

[0,0,1] axis, which has a periodicity as long as 70.8 times the Cu^{2+} spacing or 21.4 nm. This periodicity is typical for spin spirals due to relativistic, for instance, Dzyaloshinskii-Moriya (DM) interaction.¹¹ The magnetic propagation vector is expressed through reciprocal lattice vectors \mathbf{a}^* , \mathbf{b}^* , and \mathbf{c}^* as

$$\mathbf{k} = (\mathbf{a}^* + \mathbf{b}^*)/3 + 0.085\mathbf{c}^*. \quad (1)$$

The magnetic moment of Cu^{2+} at $T=0$ is determined by extrapolation to be $0.61(1)\mu_B$, a typical value for Cu^{2+} ions (see, for instance, Ref. 12). Further investigation has revealed a sixfold helical modulation corresponding to the number of Cu^{2+} planes in the chemical unit cell,¹³ with a single antiferromagnetic bond being turned by 60° from one copper layer to another, thus providing a spatial frustration. According to Ref. 13 and our preliminary results of a neutron-polarization analysis,¹⁴ this modulation results in a series of weak magnetic satellites (h,k,l) with $l \neq 6n+1$, which are forbidden in the model put forward in Ref. 6. The spin structure reconstructed by us from the measured intensities of all magnetic reflections by use of a neutron-polarization analysis will be published elsewhere. We restrict ourselves here discussing the structural data obtained at both sides of T_N . Structural studies resolving the spin ordering are highly desirable due to the suggested deviation^{13,14} from the simple helix.⁶ This deviation, the anomalous critical behavior of the specific heat,¹⁵ and NMR data¹⁶ indicate a possible structural phase transition at T_N .

The CsCuCl_3 crystal investigated in this work was grown as those studied previously by specific heat¹⁵ and neutron scattering.¹⁴ An interesting feature of this material, mentioned already in Refs. 6, 13, and 14, is the very small content of the $P6_522$ enantiomer. The population of the $P6_122$ domains was found to be 88(2)% in Ref. 14. The crystal investigated here, with volume of about $6 \times 6 \times 6$ mm³, contains 99.90(4)% of $P6_122$ domains, the origin of which is unclear so far.

The temperature dependence of the lattice parameters was investigated on the powder diffractometer at the WWR-M reactor at PNPI, Gatchina by longitudinal scans of the two reflections (0,0,24) and (4,4,1). The neutron wavelength was $\lambda = 1.3584$ Å. A fine collimation and quite large take-off angle after the monochromator have provided a good precision in the lattice parameters. In particular, we obtained a relative standard deviation of $\sigma(c)/c \approx 10^{-4}$. The temperature dependences $c(T)$ and $a(T)$, shown in Fig. 3, evidence a first-order structural transition at T_N . This observation indeed explains the earlier specific-heat results,¹⁵ where a crossover to first-order behavior was found very close of T_N .

For the structure refinement, the intensities of the nuclear Bragg reflections on both sides of T_N have been collected by ω scans using the inclined-detector diffractometer D23 installed at a thermal-neutron guide of the Institute Laue Langevin (ILL) reactor. Altogether 942 and 1372 Bragg peaks (among them 852 and 1247 nonequivalent reflections) have been measured at 2 and 15 K, respectively. The neutron wavelength used was $\lambda = 1.2734$ Å. After correction for the Lorentz and polarization factors these reflections have been used in the structure refinement. In addition to the atomic

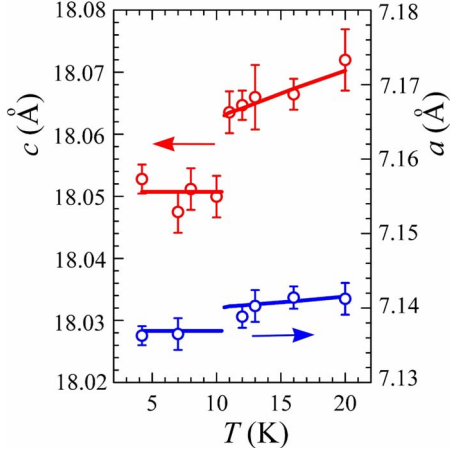


FIG. 3. (Color online) Temperature dependences of the hexagonal unit-cell lattice parameters a and c . Both dependences are obtained during heating.

coordinates and Debye-Waller factors, the population n_R of the clockwise domains, $P6_122$, has been refined. This enters the structure factor of a reflection at the momentum transfer \mathbf{Q} by

$$F(\mathbf{Q}) = n_R F_R(\mathbf{Q}) + (1 - n_R) F_L(\mathbf{Q}), \quad (2)$$

where $F_R(\mathbf{Q})$ and $F_L(\mathbf{Q})$ are the structure factors for the space groups $P6_122$ and $P6_522$, respectively. The calculated intensities $I_{\text{calc.}}(\mathbf{Q})$ are obtained from $F(\mathbf{Q})$ by

$$I_{\text{calc.}}(\mathbf{Q}) = A F(\mathbf{Q}) [1 + x F(\mathbf{Q})]^{-1/2}, \quad (3)$$

where A is a scale factor. The extinction correction x , refined simultaneously with the other parameters, is found to be small, $x=0.0541(3)$ and $x=0.0539(2)$ at 2 and 15 K, respectively. Erroneous effects can result from double Bragg scattering. This is important for the very weak reflections which could be essentially contaminated by double-scattering processes when strong reflections are involved. We got rid of this effect by excluding all weak reflections with intensities being five standard deviations stronger than $I_{\text{calc.}}$. After repeating this procedure several times, the number of used Bragg reflections reduced to 871 and 1183 for 2 and 15 K, respectively, improving the fit quality from $\chi^2 \approx 20$ to $\chi^2 \approx 1$. The refinement results are collected in Table I.

Taking into account that the high-temperature phase

TABLE I. Atomic positions x/a , y/b , and z/c and isotropic Debye-Waller factors, W , as determined from single-crystal neutron diffraction for CsCuCl_3 at 2 and 15 K in the frame of space group $P6_122$ ($Z=6$). The fraction of the $P6_122$ domains is 99.90(4)%. The fit quality is characterized by $\chi^2=1.13$, $R_w=0.053$, and $\chi^2=1.18$, $R_w=0.054$ for 2 and 15 K, respectively.

		$T=2$ K				$T=15$ K			
		$a=b=7.1369(8)$ and $c=18.0507(8)$				$a=b=7.1408(8)$ and $c=18.0666(8)$			
		x/a	y/b	z/c	W	x/a	y/b	z/c	W
Cs	$6b$	0.708 97(7)	0.354 48(4)	1/12	2.21(1)	0.709 15(7)	0.354 57(4)	1/12	1.70(1)
Cu	$6a$	0.057 96(5)	0	0	0.00(1)	0.059 23(5)	0	0	0.00(1)
Cl1	$6b$	0.766 83(7)	0.883 42(4)	1/12	0.93(1)	0.766 14(7)	0.883 07(3)	1/12	0.86(1)
Cl2	$12c$	0.355 50(3)	0.209 48(4)	0.242 24(4)	0.93(1)	0.356 11(3)	0.207 83(4)	0.242 60(3)	0.86(1)

TABLE II. Interatomic distances (\AA) and angles ϕ (deg) of the superexchange bonds at $T=2$ K $< T_N$ and $T=15$ K $> T_N$ together with the differences $\Delta_R=R(2$ K) $-R(15$ K) and $\Delta_\phi=\phi(2$ K) $-\phi(15$ K).

Bond parameters	2 K	15 K	Δ_R and Δ_ϕ
Cu-Cl1			
$R(\text{Cu}, \text{Cl1})$	2.3544(5)	2.3659(4)	-0.0115(6)
$\phi(\text{Cu}, \text{Cl1}, \text{Cu})$	80.32(2)	79.98(2)	+0.34(3)
Cu-Cl1-Cl2-Cu			
$R(\text{Cu}, \text{Cl1})$	2.3544(5)	2.3659(4)	-0.0115(6)
$R(\text{Cl1}, \text{Cl2})$	3.8796(7)	3.8616(7)	+0.018(1)
$R(\text{Cl2}, \text{Cu})$	2.2898(4)	2.2925(5)	-0.0027(6)
$\phi(\text{Cu}, \text{Cl1}, \text{Cl2})$	134.09(2)	134.26(2)	-0.17(4)
$\phi(\text{Cl1}, \text{Cl2}, \text{Cu})$	134.56(2)	134.91(2)	-0.35(5)

$P6_3mc$ is polar, we repeated the refinement below T_N assuming the space group $P6_1$, the highest polar subgroup of $P6_122$. The fit quality was very close to that of the nonpolar model. However, electrical investigations of the crystal performed in the group of Palstra (Zernike Institute for Advanced Materials, University of Groningen, The Netherlands) failed to discover neither a divergence of the dielectric constant nor an electric-field-induced polarization. Therefore, we conclude that the spin ordering is accompanied by an isostructural transition within the same space group $P6_122$.

The interatomic distances and the bond angles important for the superexchange are compared in Table II for the two temperatures used in our investigation. The copper ions may be considered as coordinated by four chlorines⁵ situated roughly on the axes ξ and η of an octahedron (ξ, η, ζ), with two remaining chlorines at sufficiently larger distances 2.78 \AA along the ζ axis, building the bond Cu-Cl1-Cu between neighboring Cu^{2+} ions along the c axis. The ground state of the Cu^{2+} ions in this coordination is B_{1g} ,¹⁷ with the wave function being expressed as

$$\psi_{1g}^{(0)} = [\beta] d_{(\xi^2 - \eta^2)}, \quad (4)$$

where the Pauli matrix $[\beta]$ corresponds to $S=-1/2$. The spin-orbit coupling modifies the wave function, but taking

into account that the ratio of the coupling constant λ to the energies of the excited levels is less than 7×10^{-2} ,¹⁷ this can be neglected.

According to the Goodenough-Kanamori rules,⁸ the superexchange interaction J (mediated by the bond Cu-C11-Cu) is ferromagnetic and strongest at $\phi=90^\circ$, which is the case for the wave function (4). The four-center in-plane superexchange interaction J' (Cu-Cl2-C11-Cu), expected to be antiferromagnetic,¹⁰ includes the overlaps Cu-Cl2, Cl2-C11, and C11-Cu. The exchange parameter $J=2.4$ meV is found from the magnon dispersion to be about six times stronger than $J'=-0.4$ meV.¹² The in-plane antiferromagnetic interaction J' does not belong to a single triangle of Cu^{2+} ions but is distributed over the pairs of ions along one of the directions [100], [110], [010], [100], [110], and [010], turning by 60° between neighboring copper layers along the c axis. Six antiferromagnetic bonds are coupled by the ferromagnetic interaction J via the C11 ions. This ferromagnetic bond provides an unusual “spatial” frustration distributed over the unit cell. (Normally a frustration appears solely due to competition of antiferromagnetic interactions.)

Actually, $J \approx 6|J'|$, which is common to all bonds, is responsible for the magnetic ordering in the unit cell. (The spiral with periodicity $\sim 12c$ is due to an antisymmetric part of the interaction provided by this link.) When inspecting Table II, one may conclude that the structural phase transition in CsCuCl_3 is accompanied by an increase in J due to the decrease in the C11-Cu distance by $0.0115(6)$ Å below T_N , which minimizes the exchange energy. The interaction mu^2 between the magnetic subsystem and the lattice, where m and u are the magnetic and the lattice degrees of freedom,

can couple the magnetic and structural phase transitions. This may change the phase transition from second order to first order if the magnetostrictive coupling due to the fluctuations is strong. However, the crossover from second- to first-order behavior can also be caused by other reasons. The first-order behavior of the specific-heat anomaly has been observed only very close to the phase transition, $5 \times 10^{-5} < |\tau| < 5 \times 10^{-3}$, where $\tau=(T-T_N)/T_N$. This means that the crossover is most probably due to long-range fluctuations. The natural long length scale in CsCuCl_3 is the helix periodicity of 21.4 nm.⁶ As mentioned previously,¹⁴ the Dzyaloshinskii vector, D , according to Ref. 18 should be inclined by an angle of 81.6° with respect to the c axis, with the D_{xy} components for the nearest copper layers making an angle of 60° . The resulting weak in-plane anisotropy seems to be the reason for the occurrence of the first-order transition.

In conclusion, we have discovered an isostructural transition coupled to the spin ordering in CsCuCl_3 —an unusual, spatially frustrated spiral crystal lattice. As far as such a transition that minimizes the exchange energy due to spin-orbit coupling has been observed for a number of lattices with largely different topology, this proves the crucial role of weak perturbations in the magnetic ordering of geometrically frustrated systems.

We acknowledge A. I. Sokolov, T. T. M. Palstra, S. V. Maleyev, and Yu. P. Chernenkov for helpful discussions, N. Mufti and U. Adem for the electrical measurements, and the Program on Low-Temperature Quantum Phenomena of the Russian Academy of Science for financial support.

*plakhty@npi.spb.ru

¹Y. Yamashita and K. Ueda, Phys. Rev. Lett. **85**, 4960 (2000).

²O. Tchernyshyov, R. Moessner, and S. L. Sondhi, Phys. Rev. Lett. **88**, 067203 (2002); Phys. Rev. B **66**, 064403 (2002).

³S. Lee, A. Pirogov, M. Kang, K. H. Jang, M. Yonemura, T. Kamiyama, S.-W. Cheong, F. Gozzo, N. Shin, H. Kimura, and J.-G. Park, Nature (London) **451**, 805 (2008).

⁴M. F. Collins and O. A. Petrenko, Can. J. Phys. **75**, 605 (1997).

⁵A. W. Schlueter, R. A. Jacobson, and R. D. Rundle, Inorg. Chem. **5**, 277 (1966).

⁶K. Adachi, N. Achiwa, and M. Mekata, J. Phys. Soc. Jpn. **49**, 545 (1980).

⁷C. J. Kroese, W. J. A. Maaskant, and G. C. Verschoor, Acta Crystallogr., Sect. B: Struct. Crystallogr. Cryst. Chem. **30**, 1053 (1974).

⁸J. B. Goodenough, *Magnetism and the Chemical Bond* (Interscience, New York, 1963).

⁹A. J. C. Wilson, *International Tables for Crystallography* (Kluwer Academic, Dordrecht, 1995), Vol. A.

¹⁰W. Geertsma and C. Haas, Physica B **164**, 261 (1990).

¹¹I. E. Dzyaloshinskii, Zh. Eksp. Teor. Fiz. **46**, 1420 (1964) [Sov. Phys. JETP **19**, 960 (1964)]; Zh. Eksp. Teor. Fiz. **47**, 336 (1964) [Sov. Phys. JETP **20**, 223 (1965)]; Zh. Eksp. Teor. Fiz. **47**, 992 (1964) [Sov. Phys. JETP **20**, 665 (1965)].

¹²I. W. Sumarlin, J. W. Lynn, T. Chattopadhyay, S. N. Barilo, D. I. Zhigunov, and J. L. Peng, Phys. Rev. B **51**, 5824 (1995).

¹³M. Mekata, Y. Ajiro, T. Sugino, A. Oohara, K. Ohara, S. Yasuda, Y. Oohara, and H. Yoshizawa, J. Magn. Magn. Mater. **140-144**, 1987 (1995).

¹⁴V. P. Plakhty, J. Wosnitza, J. Kulda, Th. Brueckel, W. Schweika, D. Visser, S. V. Gavrilov, E. V. Moskvina, R. K. Kremer, and M. G. Banks, Physica B **385-386**, 288 (2006).

¹⁵H. B. Weber, T. Werner, J. Wosnitza, H. v. Löhneysen, and U. Schotte, Phys. Rev. B **54**, 015924 (1996).

¹⁶A. R. Lim and S. H. Kim, J. Appl. Phys. **101**, 083519 (2007).

¹⁷R. Laiho, M. Natarajan, and M. Kaira, Phys. Status Solidi A **15**, 311 (1973).

¹⁸A. I. Moskvina and I. G. Bostrem, Fiz. Tverd. Tela **19**, 2616 (1977); Sov. Phys. Solid State **19**, 1532 (1977).